IEEE Access
Multidisciplinary ⋮ Rapid Review ⋮ Open Access Journal

Received April 13, 2020, accepted April 26, 2020, date of publication May 7, 2020, date of current version May 21, 2020.

Digital Object Identifier 10.1109/ACCESS.2020.2993061

Frequency Oscillation Analysis of Power System With Multiple Governor Deadbands

CHENGWEI FAN, GANG CHEN, ZHEN CHEN, HUABO SHI, CHANG LIU, AND YUFEI TENG
State Grid Sichuan Electric Power Research Institute, Chengdu 610041, China

Corresponding author: Zhen Chen (chenzhen5840@163.com)

This work was supported by the Science and Technology Project of State Grid Corporation of China "Coordination Strategy and Demonstration of Multi-stage Frequency Regulation for Large HVDC Export Power System with High Proportion of Hydropower" under Award 521999190008.

ABSTRACT In recent years, the ultra-low frequency oscillation of power system is one of the most concerned frequency stability problem. The governor deadband are considered as one of the main influences. However, the existing methods can only deal with single deadband segment. As for a multi-machine system with multiple deadband segments, it lacks the analysis method for frequency oscillation. To solve this problem, this paper first define the extended description function applied to nonlinear composite system according to the principle of traditional description function method. The extended description function can quantify the relationship of input and output of a system with multiple nonlinear segments. Then, based on the uniform frequency model of multiple governors, the turbines and governors of hydro and thermal power units with different deadband widths are equivalent to one extended description function. The locus of minus reciprocal of the extended description function with oscillation amplitude and the Nyquist curve of the generator are plotted on the complex plane for the analysis of system stability. Next, the critical oscillation amplitude of disturbance to trigger the system frequency oscillation is calculated according to the point of intersection of both curves. Finally, the simulation results show that the critical oscillation amplitude can reflect the stability of system. The change of deadband width is positively correlated with the critical oscillation amplitude. The appropriate setting of deadband and configuration of hydro-thermal generation are effective measures to suppress the ultra-low frequency oscillation while retain the ability of frequency regulation.

INDEX TERMS Ultra-low frequency oscillation, multiple governor deadbands, nonlinear composite system, extended description function.

I. INTRODUCTION

The development of direct current (DC) transmission project has promoted the transition from synchronous interconnection to asynchronous interconnection of regional power grids in China. One of the main problems from the transition is the prominent frequency instability, especially the ultra-low frequency oscillation [1]–[3]. Take the Southwest Grid in China as an example [4]. After the back-to-back DC project for the Southwest and Central China Connection began operation, the Southwest Grid is asynchronously isolated. The capacity of generation is only 1/5 as that in synchronous interconnection. The decline of frequency due to disturbance is fast so the parameters of all governors are adjusted for fast regulation. As a result, an ultra-low frequency oscillation of 0.05 Hz occurs in the quasi steady state after the governor regulation.

The common method applied in the mechanism study of ultra-low frequency oscillation is to use a low-order system frequency response (SFR) model as the equivalent model to the whole power system [5], [6]. Reference [7] makes a regional power grid become equivalent to a SFR model of single-machine with multiple governors. The equivalent SFR model consists of main governors and prime movers connected to the regional grid and is a high-order linear system. By calculation the eigenvalue of the equivalent model, the influence of hydro-thermal power ratio and hydro governor parameters on the ultra-low frequency oscillation is analyzed. However, the eigenvalue computation of a high-order system is already difficult, especially considering the eigenvalue

The associate editor coordinating the review of this manuscript and approving it for publication was Yunfeng Wen.

change caused by the variation of governor parameters. In order to derive the analytical solution of oscillation frequency and damping of a single-machine system with load model, Reference [8] simplifies the governor to a regulation coefficient. It focuses on how the turbine parameters and the power-frequency characteristic of load affect the damping ratio. Reference [9] considers the power-voltage characteristic of load and system power loss in the established single-machine single-load SFR model of multiple governors. The eigenvalue analysis of the improved model indicates that the consideration of the two conditions produces a better stability of power system. So it follows that the ignorance of the two conditions brings forth more conservative but secure result. Reference [10] establishes the SFR model consisting of hydro and thermal power governors. It defines the minimum distance from the system Nyquist curve to the point $(-1, 0)$ in the complex plane as the stability margin. By analyzing the influence of hydro and thermal power respectively on the minimum distance, the contribution of each to the system stability is presented. Reference [11] proves that the parameters of hydro governor leading to system negative damping are the main cause of ultra-low frequency oscillation. It specifically puts forward a method of withdrawing a portion of hydropower units and optimizing the governor deadbands to suppress the ultra-low frequency oscillation.

The idea of applying the describing function method to overcome nonlinearity is proposed in the oscillation analysis of power system [12], [13]. The accuracy and completeness of stability analysis is proven to be enhanced. Regarding the influence of deadband, Reference [14] firstly introduce the governor deadband into the ultra-low frequency oscillation analysis. The ultra-low frequency oscillation occurs when the system is subjected to a certain magnitude of power disturbance according to the Nyquist criterion. But this method is only applicable to a system with one single deadband due to the restriction of description function method. Reference [15] proposes further on a numerical analysis method to deal with a system with multiple deadbands. The main idea is to combine the locus of eigenvalue with the describing function method. In each step of locus, the describing function of deadband is a constant real number. The computation of multiple nonlinearities are thus avoided. However, the difficulty of computing the eigenvalue of high-order system repeatedly is still a problem. Besides, the accuracy depends on the step of frequency amplitude.

Besides the SFR based method, the state-space method and the energy function method are available. The state-space method is based on the linear model and fully involves the correlation of generation-transmission-load, while the difficulty of modeling and computation is high when applicable in a complex system [16]. The energy function method is in consistent with the damping torque method. Combined with the measurements from PMU equipment, it is feasible to evaluate the damping characteristic of governor online [17].

Based on the existing researches, the following conclusions can be drawn. Firstly, all generators are synchronous in the ultra-low frequency oscillation. Secondly, the hydropower unit deteriorates the frequency stability of power system while the thermal power enhances it. Thirdly, the governor deadband make it complicated to analyze the system stability. The governor deadband exists extensively in the practical power grid and the deadband width is different. Therefore, on the basis of existing methods, this paper adopts the extended describing function method and the Nyquist stability criterion to calculate the critical magnitude of frequency disturbance to cause oscillation. The critical magnitude is an indicator of system frequency stability. The influence of multiple governor deadbands on frequency oscillation is quantitatively evaluated.

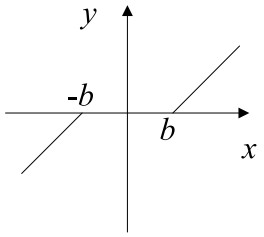

FIGURE 1. Non-step deadband.

II. NONLINEAR COMPOSITE SYSTEM

Reference [14] studies the influence of step, non-step and hysteresis deadband on the frequency oscillation based on the single-machine system with single governor. The main kind of governor deadband in both the practical system and the simulation model of power company is non-step deadband. Given the situation, this paper focuses on the non-step kind of deadband as shown in Fig. 1.

The hydro and thermal power generations are the main kind of sources in the practical power grid. The settings of governor deadband for the two kinds are quite different. Fig. 2 shows the diagram of a SFR model. It contains a hydro turbine-governor and a thermal turbine-governor along with each deadband segment. The generators all maintain synchronous in the ultra-low frequency oscillation, so an equivalent machine of inertial center is adopted.

Ignore the system power loss and consider the power-frequency characteristic of load and generator damping, the transfer function of the equivalent machine is

$$G_{\text{gen}} = \frac{1}{T_{\text{J}}s + D_{\text{s}}} \tag{1}$$

where T_{J} is the rotational inertia, and D_{S} is the sum of generator damping coefficient and load power-frequency coefficient.

The hydro turbine-governor model is referred from Reference [14], and is expressed as Equation (2) and Equation (3).

$$G_{\text{ht}} = \frac{1 - T_{\text{W}}s}{1 + 0.5T_{\text{W}}s} \tag{2}$$

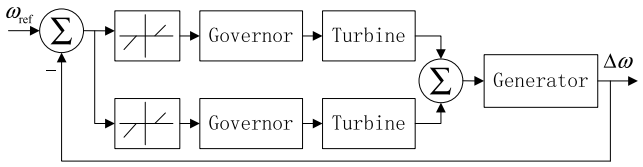

FIGURE 2. System model.

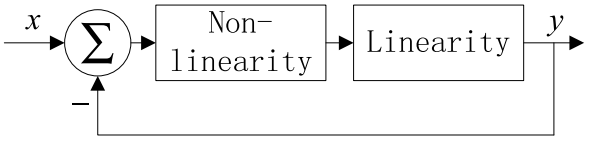

FIGURE 3. Typical single-nonlinear-segment system.

$$G_{\text{hgov}} = \frac{K_{\text{D}}s^2 + K_{\text{P}}s + K_{\text{I}}}{B_{\text{P}}K_{\text{I}} + s} \cdot \frac{1}{1 + T_{\text{G}}s} \tag{3}$$

where T_{W} is the time constant of water hammer effect, K_{D}, K_{P} and K_{I} are the differential, proportional and integral coefficients respectively, B_{P} is the regulation coefficient, T_{G} is the time constant of servosystem.

The steam turbine-governor model is referred from Reference [10], and is expressed as Equation (4) and Equation (5).

$$G_{\text{st}} = \frac{1 + F_{\text{HP}}T_{\text{RH}}s}{(1 + T_{\text{CH}}s)(1 + T_{\text{RH}}s)} \tag{4}$$

$$G_{\text{sgov}} = \frac{1}{R} \cdot \frac{1}{1 + T_{\text{G}}s} \tag{5}$$

where F_{HP} is the ratio of high pressure cylinder power in the total turbine power, T_{RH} is the reheat time constant, T_{CH} is the time constant of air intake volume.

The system shown in Fig. 2 is nonlinear. The hydro and thermal governor contain different widths of deadband, so they should be regarded as two individual nonlinear segments. Except that, the turbine-governor and generator are all linear. The whole system is a typical nonlinear composite system. The conventional describing function method can only deal with a system with one single nonlinear segment as shown in Fig. 3, or a system of multiple nonlinear segments with no linear segment interleave.

III. EXTENDED DESCRIBING FUNCTION METHOD

The describing function method uses the fundamental harmonic to approximate the nonlinear segment output given the input of a sinusoidal signal [18]. Given a sinusoidal input, the output of the nonlinear segment is expanded by the Fourier series. The complex-valued ratio of the output fundamental component to the sinusoidal input is the describing function of the nonlinear segment. It can be regarded as a variable gain of its input as a substitution of nonlinear segment [19]. It is applicable to analyze the oscillation in the critically stable state. For a nonlinear composite system, the multiple nonlinear segments make it difficult to apply the describing function method directly. In order to ascertain the input-output relation of a nonlinear composite system,

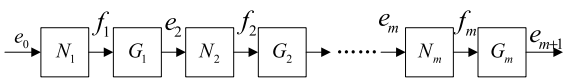

FIGURE 4. Simple nonlinear composite system.

the describing function method is improved. Firstly, each nonlinear segment is expressed by a conventional describing function. Secondly, the whole system input-output relation is obtained through the vector calculation algorithm. Finally, an extended describing function to substitute the whole nonlinear composite system is obtained [20].

Take the simple nonlinear composite system in Fig. 4 as an example. $N_1 \sim N_m$ are describing functions for each individual nonlinear segment. $G_1 \sim G_m$ are transfer functions of linear parts. The starting input signal is expressed as

$$e_0 = A_0 \sin(\omega t + \theta_0) \tag{6}$$

The input for each nonlinear segment can be expressed as

$$\begin{cases} e_2 = A_2 \sin(\omega t + \theta_2) \\ e_3 = A_3 \sin(\omega t + \theta_3) \\ \vdots \\ e_{m+1} = A_{m+1} \sin(\omega t + \theta_{m+1}) \end{cases} \tag{7}$$

So the input for each linear segment, which is also the output of each nonlinear segment, is expressed as

$$\begin{cases} f_1 = A_0 \left|N_1(A_0)\right| \sin(\omega t + \theta_0 + \angle N_1(A_0)) \\ f_2 = A_2 \left|N_2(A_2)\right| \sin(\omega t + \theta_2 + \angle N_2(A_2)) \\ \vdots \\ f_m = A_m \left|N_m(A_m)\right| \sin(\omega t + \theta_m + \angle N_m(A_m)) \end{cases} \tag{8}$$

where

$$\begin{cases} A_2 = A_0 \left|N_1(A_0)\right| \left|G_1(j\omega)\right| \\ A_3 = A_2 \left|N_2(A_2)\right| \left|G_2(j\omega)\right| \\ \vdots \\ A_{m+1} = A_m \left|N_m(A_m)\right| \left|G_m(j\omega)\right| \end{cases} \tag{9}$$

$$\begin{cases} \theta_2 = \angle N_1(A_0) + \angle G_1(j\omega) \\ \theta_3 = \theta_2 + \angle N_2(A_2) + \angle G_2(j\omega) \\ \vdots \\ \theta_{m+1} = \theta_m + \angle N_m(A_m) + \angle G_m(j\omega) \end{cases} \tag{10}$$

The amplitude and phase angle of the extended describing function is defined as $|G_{\text{e}}(A_0, \omega)|$ and $\angle G_{\text{e}}(A_0, \omega)$ respectively.

$$\begin{aligned} |G_{\text{e}}(A_0, \omega)| &= \left|\frac{e_{m+1}}{e_0}\right| = \frac{A_{m+1}}{A_0} \\ \angle G_{\text{e}}(A_0, \omega) &= \angle\frac{e_{m+1}}{e_0} = \theta_{m+1} - \theta_0 \end{aligned} \tag{11}$$

For a nonlinear composite system shown in Fig. 4, the extended describing function $G_{\text{e}}(A_0, \omega)$ represents the input-output relation. Use $G_{\text{e}}(A_0, \omega)$ to substitute the whole

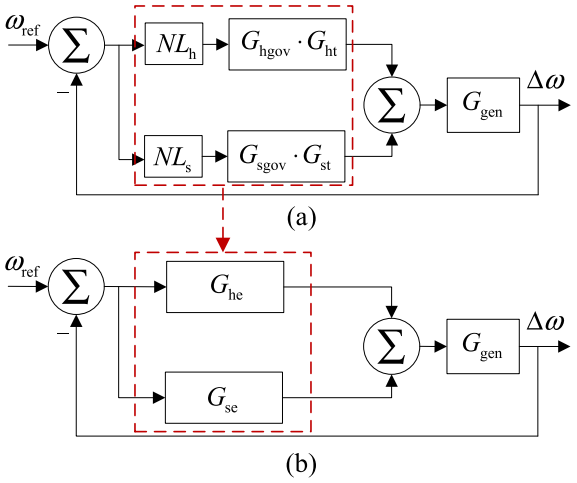

FIGURE 5. Transfer function graph of system with multiple deadbands.

nonlinear composite system, the stability analysis can be implemented.

IV. ANALYSIS OF MULTIPLE DEADBAND SEGMENTS IN MULTI_MACHINE SYSTEM

Different deadband widths, governor models and parameters make it a nonlinear composite system in Fig. 2, on which the conventional describing function method cannot be applied. Fig. 5(a) shows the transfer function graph of the example system. NL_h and NL_s are the describing functions of hydro and thermal governors respectively. By using the method proposed in Section 3, each branch in Fig. 5 (a) is equivalent to an extended describing function as shown in Fig. 5(b). G_{he} and G_{se} represent the extended describing functions of hydro and thermal power. Then, using the idea of combination algorithm from the conventional describing function method, the multi-branch system is equivalent to the form shown in Fig. 3. The stability analysis is implemented based on its Nyquist curve. All the curves depicted in this section are based on the parameters from Section V.A.

A. EXTENDED DESCRIBGING FUNCTION OF SINGLE BRANCH

First analyze the hydro governor branch. The describing function of the non-step deadband segment is

$$NL_h = \frac{2}{\pi}\left(\frac{\pi}{2} - \sin^{-1}\left(\frac{b_1}{A_0}\right) - \frac{b_1}{A_0}\sqrt{1-\left(\frac{b_1}{A_0}\right)^2}\right) \quad (12)$$

where b_1 is the deadband width, A_0 is the disturbance magnitude.

The deadband segment and the governor are connected in series. According to the method proposed in Section 3, the extended describing function amplitude and phase angle of the hydro governor with deadband are

$$\begin{aligned} |G_{he}(A_0,\omega)| &= |NL_h|\,|G_{hgov}\cdot G_{ht}| \\ \angle G_{he}(A_0,\omega) &= \angle NL_h + \angle G_{hgov}\cdot G_{ht} \end{aligned} \quad (13)$$

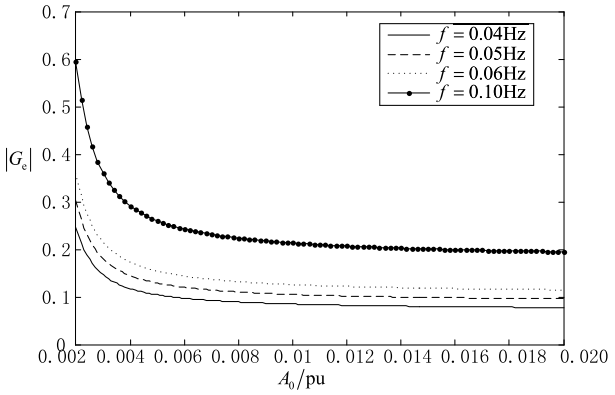

FIGURE 6. Calculated amplitude characteristics of the extended description function.

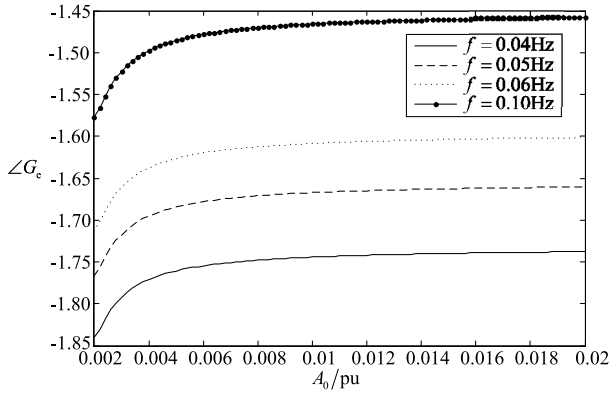

FIGURE 7. Calculated angle characteristics of the extended description function.

Likewise, the extended describing function G_{se} of thermal governor with deadband can be obtained.

B. COMBINATION OF MULTIPLE BRANCHES

Similar to the conventional describing function method, the two paralleled branches of nonlinear system share the same input and their output are added together according to the combination algorithm. So the entire nonlinear system is equivalent to the algebraic addition of the two extended describing functions.

$$G_e = G_{he} + G_{se} \quad (14)$$

G_e is the function of disturbance magnitude A_0 and rotation speed ω. Given different frequency f ($\omega = 2\pi f$), the curves of amplitude and phase angle changing with A_0 are presented in Fig. 6 and Fig. 7.

C. DEADBAND INFLUENCE ANALYSIS

After the extended describing function of multi-deadband is obtained, the curve of $-1/G_e(A_0)$ along with A_0 increasing from the value of deadband width can be depicted. Similarly, the value of ω is determined according to $\omega = 2\pi f$ for each curve of $-1/G_e(A_0)$. Combined with the Nyquist Curve of generator $G_{gen}(s)$, the system stability can be analyzed.

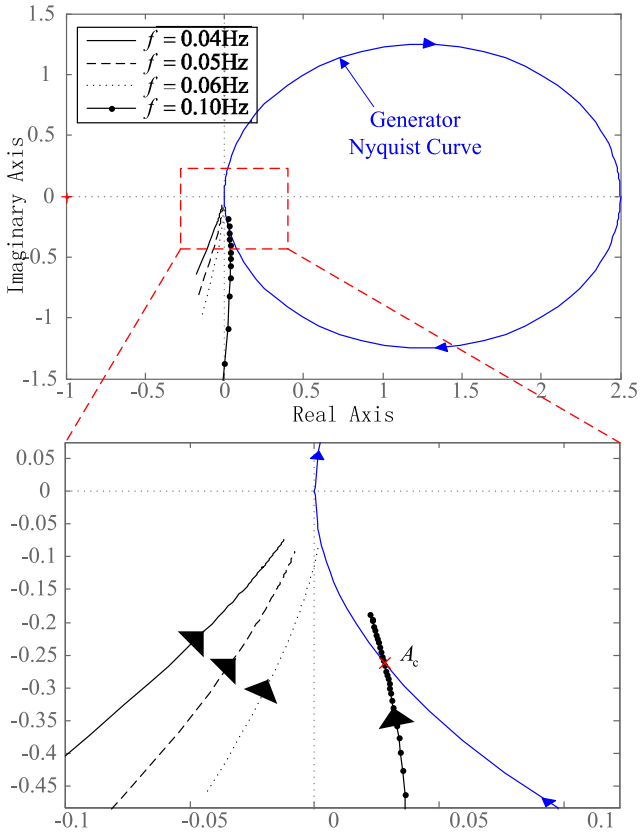

FIGURE 8. Open-loop frequency characteristics and negative reciprocal of extended description function.

As the oscillation frequency value is different, the negative reciprocal curve of the extended describing function G_e and the Nyquist curve of generator intersect differently. In Fig. 8, the arrowhead indicates the change direction of the $-1/G_e$ curve with the increase of A_0. As the $-1/G_e$ curve and the generator Nyquist curve do not intersect, the nonlinear system is stable. As they do, the point of intersection corresponds to a critical amplitude A_0. When a disturbance of over A_0 amplitude occurs, the system becomes instable, otherwise stable.

Similarly given $A_0 = 0.01$pu and $f = 0.1$Hz, the influence of deadband width change on the system stability is analyzed. The deadband widths of hydro and thermal governors are set to be $0.0020 + b$ and $0.0015 + b$ respectively. Then the extended describing function G_e is a function of b. The curve of $-1/G_e(b)$ is depicted in Fig. 9 along with the Nyquist curve of generator. The arrowhead indicates the change direction of $-1/G_e(b)$ with b increasing from 0. Shown in Fig. 9, $-1/G_e(b)$ is initially encircled by the generator Nyquist curve and the system is instable. While b increases from 0, $-1/G_e(b)$ passes through the Nyquist curve and the system is brought into the stable area. Therefore, it can be concluded that in regard to frequency oscillation, the system stability becomes higher with the increase of deadband width.

Note that in Fig. 8 and Fig. 9, the intersection point corresponds to different oscillation frequency ω for G_e and G_{gen}. While in a connected system, they are of the same frequency

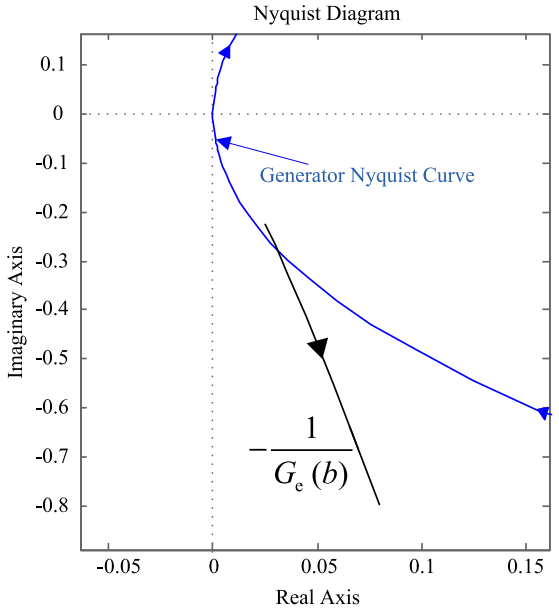

FIGURE 9. Negative reciprocal of extended description function changing with deadband width.

ω. The key point of Fig. 8 and Fig. 9 is to indicate that there exists an unknown point where G_e and G_{gen} can intersect with the same frequency. Then it leads to the purpose of proposed method to locate the point, that is to solve the critical amplitude A_0 and oscillation frequency ω_0.

The value of critical amplitude A_0 is the key to the analysis of ultra-low frequency oscillation. The intersection point of both curves corresponds to the limit cycle, the creation condition of which is

$$\begin{aligned} |G_e| \cdot |G_{gen}| &= 1 \\ \angle G_e + \angle G_{gen} &= -\pi/2 \end{aligned} \tag{15}$$

To solve the simultaneous equations (15) provides the critical amplitude A_0 and its corresponding oscillation frequency ω_0. The high value of A_0 indicates that the amplitude of disturbance to cause the ultra-low frequency oscillation is high, so is the system stability. Hence, the value of critical amplitude A_0 is a measure of the system stability.

V. SIMULATION

A. SYSTEM DESCRIPTION

This section adopts the system in Fig. 2 to verify the proposed method. The configuration parameters are as follows.

Generator parameters: $T_J = 10.0s$, $D_S = 0.4$.

Hydro turbine G_{ht} and governor G_{hgov} parameters: $K_P = 0.5$, $K_D = 0.7$, $K_I = 1$, $T_W = 1$, $T_{gh} = 0.2$, $b_p = 0.04$.

Thermal turbine G_{st} and governor G_{sgov} parameters: $R = 0.0303$, $T_{gg} = 0.2$, $F_{hp} = 1$, $T_{rh} = 10$, $T_{ch} = 12$.

Moreover, b_1 and b_2 are the deadbands of hydro and thermal governors respectively. By adjusting the value of b_1 and b_2, the critical amplitudes to cause system oscillation are calculated through the proposed method. The results are presented in Table 1.

TABLE 1. A_0 results of different deadbands.

Case	Deadband(pu) b_1	Deadband(pu) b_2	A_0(pu)	Note
1	0.0020	0.0015	0.0116	Benchmark
2	0.0022	0.0018	0.0129	Increase both deadbands
3	0.0013	0.0008	0.0073	Decrease both deadbands
4	0.0017	0.0015	0.0101	Decrease hydro deadband
5	0.0020	0.0012	0.0112	Decrease thermal deadband
6	0.0015	0.0020	0.0097	Interchange

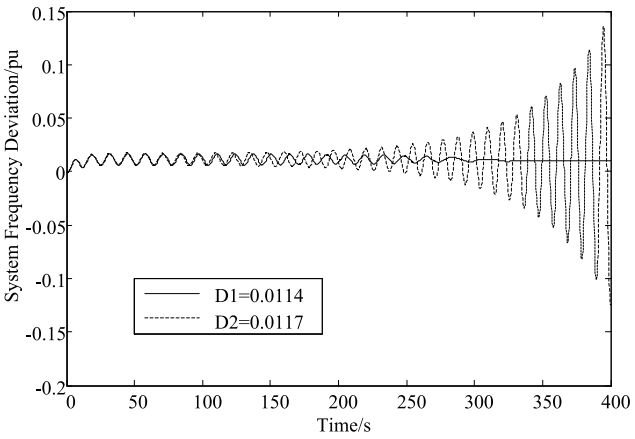

FIGURE 10. System frequency response of Case 1 with different frequency disturbances.

B. ULTRA-LOW FREQUENCY OSCILLATION ANALYSIS OF MULTI-DEADBAND SYSTEM

Focus on Case 1, 3 and 5 in this section. The deadband widths are different but within a common range in the three cases. It aims to test the effectiveness of the proposed method on different deadband widths. Establish the system of Fig. 2 in MATLAB/Simulink, set the deadband widths according to Case 1, 3 and 5, test the system with different amplitudes of disturbance, and the system stability can be observed.

Every setting of deadband in different cases corresponds to a specific critical amplitude. According to the analysis in Section IV.C, when the amplitude of disturbance is larger than the critical amplitude, the system is instable with a frequency oscillation. Otherwise, the oscillation does not last and the system is stable. The critical amplitudes are larger than the deadband widths in each case, then the two disturbances of less-than and greater-than critical amplitude (D1 and D2) are input into the system. The frequency response curves are presented in Fig. 10. In Case 1, the critical amplitude is 0.0116 pu. The disturbance of 0.0114 pu magnitude triggers a oscillation to decay gradually. The disturbance of 0.0117 pu is over the critical amplitude, so the oscillation persists to destabilize the system. The scenarios are similar in Case 3 and Case 5 and accord with the analysis in Section IV.C.

C. INFLUENCE OF DEADBAND WIDTH

The system established in Fig. 2 consists of a thermal and hydro generator, which is conducive to study the deadband influence involving the frequency regulation of different energy sources units. Case 1 is deemed as the benchmark in this section and compared with the other cases.

1) INCREASE OR DECREASE BOTH DEADBAND WIDTHS

The two deadband widths are increased (Case 2) or decreased (Case 3) together. The critical amplitude is in positive correlation with deadband width. It is related to the deadband characteristic. With a wider deadband, the range for the disturbance to go through to activate the governor regulation is larger. The critical amplitude of disturbance to trigger the ultra-low frequency oscillation is thus higher. Hence, the system stability is higher. This is consistent with the analysis in Section IV.C.

2) DECREASE THE HYDRO OR THERMAL DEADBAND WIDTH SEPARATELY

Compare the critical amplitude from Case 4 (decrease the hydro deadband) and Case 5 (decrease the thermal deadband) with that from Case 1. It can be seen from the comparison that to decrease whether the hydro or thermal deadband decreases the threshold value of disturbance amplitude to trigger frequency oscillation. The risk of system disability increases. Meanwhile, it shows that to decrease the same width (0.0003 pu), the critical amplitude of Case 5 is higher than that of Case 4. It indicates that to decrease the hydro deadband is more conducive to deteriorate the system stability than to decrease the thermal deadband.

3) INCREASE THE HYDRO DEADBAND AND DECREASE THE THERMAL DEADBAND SIMULTANEOUSLY

In order to study the influence of different participation level of hydro and thermal governor due to the deadband limit in the frequency regulation, meanwhile to exclude the influence of deadband itself on the critical amplitude explained in section (1), Case 6 exchanges the deadband setting between the hydro and thermal governor. After the exchange, there are a same deadband setting of 0.0015 pu and 0.0020 pu in both Case 1 and Case 6. The difference in Case 1 is that the thermal governor is of lower deadband width and it responses to the disturbance firstly. After a period of the thermal governor regulation, the hydro governor participates in the regulation. It is just the opposite in Case 6.

With a disturbance of 0.01 pu magnitude as input, the system frequency oscillations of Case 1 and Case 6 are opposite. Because the disturbance amplitude is less than the critical amplitude of Case 1 (0.0116 pu), the solid curve of oscillation decays. While the disturbance curve exceeds the critical amplitude of Case 6 (0.0097 pu), the dashed curve of oscillation persists.

The critical amplitude of Case 6 is less than that of Case1. It indicates that when the whole participation level of governors remains the same, to increase the participation of thermal governor and decrease that of hydro governor is conducive to suppress the ultra-low frequency oscillation. For

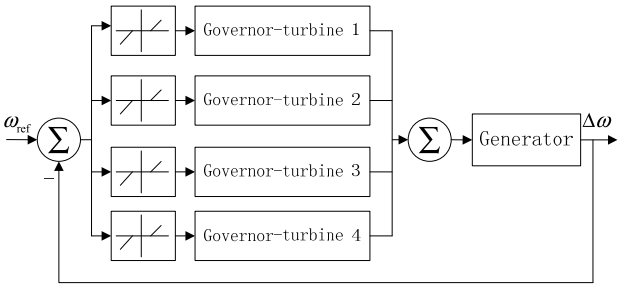

FIGURE 11. 4-governor single machine system.

TABLE 2. A_0 results of different hydro-thermal ratio.

Case	Unit Number		A_c(pu)
	Hydro	Thermal	
1	2	2	0.001930
2	3	1	0.001659
3	1	3	0.002227

the primary frequency regulation, a larger deadband width reduces the ability of system frequency regulation. Therefore, to avoid the system frequency decline significantly and also suppress the ultra-low frequency oscillation, it is practical to optimize the deadband setting of hydro and thermal governor to control the system frequency response.

D. HYDRO-THERMAL GENERATION RATIO ANALYSIS

The aim of the proposed method is to analyze a multi-machine power system with hydro and thermal generation. The previous analysis is based on a system with two units of one hydro and one thermal generation. This section focuses on the multi-machine system and the ratio of hydro and thermal generation. For this purpose, a 4-governor single-machine system is established shown in Fig. 11. Based on this model, three cases of different hydro-thermal configurations are studied.

In Case I, the system consists of two hydro units and two thermal units. In Case II, the system consists of three hydro units and one thermal unit. It is for the test of high proportion of hydro generation. In Case III, the system consists of one hydro unit and three thermal units. This case is to test the measure of increasing the thermal generation while decreasing the hydro generation to suppress the ultra-low frequency oscillation. In all cases, the hydro units share the same width of 0.0010 pu deadband and the thermal units share the other same width of 0.00080 pu deadband.

Table 2 shows the critical amplitude of three cases. It can be seen from the table that the adjustment of hydro-thermal ratio affects the critical amplitude. By inputting a disturbance of 0.002 pu, the frequency curves from Case II and Case III are presented in Fig. 12. The disturbance causes a diverging oscillation in Case II while it causes a converging oscillation in Case III. The comparison proves that the critical amplitude gives a distinct boundary of the frequency stability. The appropriate configuration of hydro-thermal generation helps enhance the stability of power system.

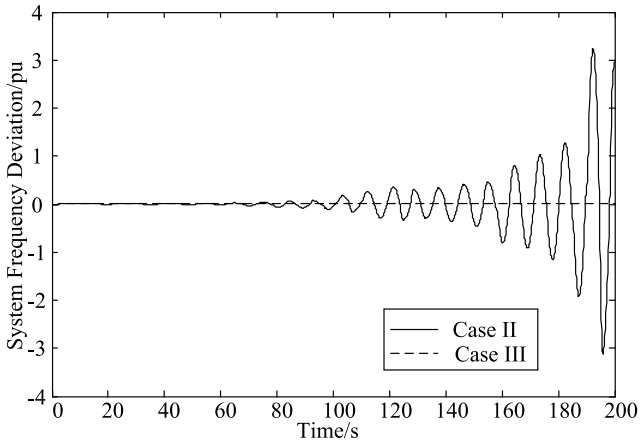

FIGURE 12. Comparison of Case II and Case III with a disturbance of 0.002 pu amplitude.

VI. CONCLUSION

The variety of deadband widths in a multi-machine system makes it infeasible to apply the traditional describing function method in analysis of ultra-low frequency oscillation. This paper proposes a novel extended describing function method, in which the nonlinear composite system of multi-deadband is equivalent to a structure of an extended describing function and a linear transfer function. Then the Nyquist curve is adopted to analyze the system stability. If the negative reciprocal curve of the extended describing function intersects with the Nyquist curve of the generator, the critical amplitude corresponding to the intersection point is the minimum value of disturbance magnitude to cause frequency instability. The simulation result proves that the critical amplitude reflects the stability level of power system. By changing the deadband setting of different generation unit, the critical amplitude is obtained. The value of critical amplitude shows that the thermal governor is more conducive than the hydro governor to suppress the ultra-low frequency oscillation. By setting the appropriate configuration of hydro-thermal generation, the frequency stability of power system can be improved meanwhile the ability of frequency regulation is maintained. The method proposed in this paper is an extension of the describing function method. It plays an important role in expanding the stability analysis range from the single-machine to multi-machine system, from the single-nonlinear segment to multi-nonlinear segment system.

REFERENCES

[1] G. Ding, A. Xue, C. Zheng, J. Wang, B. Liu, X. Zhang, and T. Bi, "Analysis of ultra-low frequency oscillation in southwest power grid based on measurement data," in *Proc. 37th Chin. Control Conf. (CCC)*, Wuhan, China, Jul. 2018, pp. 8715–8719.

[2] C. Liu, H. Shi, G. Chen, H. Zhang, X. Han, L. Ding, and C. Fan, "Governor parameters optimization strategy and support system for hydro-dominant power systems," in *Proc. Int. Conf. Power Syst. Technol. (POWERCON)*, Guangzhou, China, Nov. 2018, pp. 254–259.

[3] C. Liu, J. Zhang, J. Zhang, and C. Liu, "Mechanism and measurement of ultra-low-frequency oscillations in asynchronous networks," in *Proc. IEEE Power Energy Soc. Gen. Meeting (PESGM)*, Portland, OR, USA, Aug. 2018, pp. 1–5.

[4] X. Han, Q. Jiang, T. Liu, B. Li, L. Ding, and G. Chen, "Research on ultra-low frequency oscillation caused by hydro power in hydro-dominant power system," in *Proc. Int. Conf. Power Syst. Technol. (POWERCON)*, Guangzhou, China, Nov. 2018, pp. 1909–1914.
[5] P. M. Anderson and M. Mirheydar, "A low-order system frequency response model," *IEEE Trans. Power Syst.*, vol. 5, no. 3, pp. 720–729, Oct. 1990.
[6] X. Lu, L. Chen, Y. Zhang, Y. Min, and M. Wang, "Limit cycle in the ultra-low-frequency oscillation of islanded power systems," in *Proc. 13th IEEE Int. Conf. Control Autom. (ICCA)*, Jul. 2017, Ohrid, Macedonia, pp. 648–653.
[7] J. Zhou, "Influence of deadband of governor on frequency oscillation in single machine equivalent system," *Power Syst. Technol.*, vol. 41, no. 10, pp. 3147–3152, 2017.
[8] X. Lu, "Ultra-low-frequency oscillation of power system sprimary frequency regulation," *Autom. Electr. Power Syst.*, vol. 41, no. 16, pp. 64–70, 2017.
[9] L. Chen, "Analysis of ultra-low-frequency oscillation in multi-machine system and equivalent method," *Autom. Electr. Power Syst.*, vol. 41, no. 22, pp. 10–25, 2017.
[10] W. Huang, "Stability analysis of ultra-low frequency oscillation and governor parameter optimization for multi-machine system," *Autom. Electr. Power Syst.*, vol. 42, no. 21, pp. 185–191, 2018.
[11] W. Li, "Ultra-low-frequency Oscillation and Countermeasures in Yunnan-Guangdong UHVDC Sending-end System in Islanded Operating Mode," *Autom. Electr. Power Syst.*, vol. 42, no. 16, pp. 161–166, 2018.
[12] Y. Xia, M. Yu, X. Wang, and W. Wei, "Describing function method based power oscillation analysis of LCL-filtered single-stage PV generators connected to weak grid," *IEEE Trans. Power Electron.*, vol. 34, no. 9, pp. 8724–8738, Sep. 2019.
[13] Y. Xia, Y. Peng, P. Yang, Y. Li, and W. Wei, "Different influence of grid impedance on Low- and high-frequency stability of PV generators," *IEEE Trans. Ind. Electron.*, vol. 66, no. 11, pp. 8498–8508, Nov. 2019.
[14] L. Chen, "Influence of Deadband of Governor on Frequency Oscillation in Single Machine Equivalent System," *Autom. Electr. Power Syst.*, vol. 43, no. 7, pp. 107–128, 2019.
[15] L. Chen, Z. Lu, Y. Min, R. Yu, B. Liu, and Q. Chen, "Analysis of power system frequency oscillations with intentional governor deadbands using describing functions," *Int. J. Electr. Power Energy Syst.*, vol. 111, pp. 390–397, Oct. 2019.
[16] Y. Teng, P. Zhang, R. Han, C. Fan, X. Wang, Z. Jiang, C. Zhang, Y. Sun, Y. Gong, and J. Yi, "Mechanism and characteristics analysis of ultra-low frequency oscillation phenomenon in a power grid with a high proportion of hydropower," in *Proc. Int. Conf. Power Syst. Technol. (POWERCON)*, Guangzhou, China, Nov. 2018, pp. 575–584.
[17] L. Chen, "Online Analysis and Emergency Control of Ultra-low-frequency Oscillation Using Transient Energy Flow," *Autom. Electr. Power Syst.*, vol. 41, no. 17, pp. 9–14, 2017.
[18] K. Hassanaa Khalil, "The describing function method," in *Nonlinear Systerm*, 2nd ed. Upper Saddle River, NJ, USA: Prentice-Hall, 1996, pp. 450–468.
[19] F. Chengwei, W. Xiaoru, T. Yufei, and W. Wencheng, "Minimum frequency estimation of power system considering governor deadbands," *IET Gener., Transmiss. Distrib.*, vol. 11, no. 15, pp. 3814–3822, Oct. 2017.
[20] L. W. Taylor and J. W. Smith, "An analysis of the limit-cycle and structural-resonance characteristics of the X-15 stability augmentation system," NASA, Washington, DC, USA, Tech. Rep. NASA TN D-4287, Nov. 1967.

CHENGWEI FAN was born in Weiyuan, Sichuan, China, in 1989. He received the B.S. and Ph.D. degrees in electrical engineering from Southwest Jiaotong University, China, in 2012 and 2018, respectively.

Since 2018, he has been an Engineer with the Power System Technology Department, State Grid Sichuan Electric Power Research Institute, China. His research interests include frequency stability analysis and control of power systems.

GANG CHEN was born in 1985. He received the B.S. degree in electrical engineering from Tianjin University, Tianjin, China, in 2008, and the Ph.D. degree in electrical engineering from Tsinghua University, Beijing, China, in 2013. From September 2010 to August 2011, he was a Guest Ph.D. Student with the School of Electrical Engineering and Computer Science, Washington State University, USA. He is currently a Senior Engineer with the State Grid Sichuan Electric Power Research Institute, Chengdu, China. His research interests include power system dynamic monitoring and control based on wide-area signals, power system frequency stability analysis and control, and low and ultra-low frequency oscillation analysis and control.

ZHEN CHEN was born in Deyang, Sichuan, China, in 1991. He received the B.S. and Ph.D. degrees in electrical engineering from Sichuan University, China, in 2013 and 2017, respectively.

Since 2017, he has been a Postdoctoral Fellow jointly supervised by State Grid Sichuan Electrical Power Company and Tsinghua University. His research interests include frequency stability analysis and artificial intelligence application in power systems.

HUABO SHI was born in 1987. He received the master's degree in electrical engineering from Sichuan University, China, in 2013.

He is currently an Engineer with the State Grid Sichuan Electric Power Research Institute, Chengdu, China. His current research interest includes power system transient stability analysis and control.

CHANG LIU was born Sichuan, in 1991. She received the B.S. degree in power system and its automation from Sichuan University, Chengdu, China, in 2014, and the M.S. degree in electrical and electronic engineering from North China Electric Power University, Beijing, China, in 2017. She is currently pursuing the Ph.D. degree with the College of Electrical Engineering, Sichuan University. She is also an Assistant Engineer at the State Grid Sichuan Electric Research Institute, Chengdu, China. Her research interests mainly include stability analysis and control of power systems.

YUFEI TENG was born Sichuan, in 1984. He received the B.S. and Ph.D. degrees in electrical engineering from Xi'an Jiaotong University, Xi'an, China, in 2006 and 2012, respectively.

Since 2012, he has been with the State Grid Sichuan Electric Power Research Institute, China. From 2017 to 2019, he works as the Deputy Director of the Relay Protection and Automation Department. He is currently the Deputy Director of the Power System Technology Department. His research interests include power system stability and analysis and new transmission systems.